ACS PHYSICAL CHEMISTRY Au
AN OPEN ACCESS JOURNAL OF THE AMERICAN CHEMICAL SOCIETY

pubs.acs.org/physchemau

Article

Empirical Parameter to Compare Molecule–Electrode Interfaces in Large-Area Molecular Junctions

Marco Carlotti,[¶] Saurabh Soni,[¶] Andrii Kovalchuk, Sumit Kumar, Stephan Hofmann, and Ryan C. Chiechi*

Cite This: *ACS Phys. Chem Au* 2022, 2, 179–190

Read Online

ACCESS | Metrics & More | Article Recommendations | Supporting Information

ABSTRACT: This paper describes a simple model for comparing the degree of electronic coupling between molecules and electrodes across different large-area molecular junctions. The resulting coupling parameter can be obtained directly from current–voltage data or extracted from published data without fitting. We demonstrate the generalizability of this model by comparing over 40 different junctions comprising different molecules and measured by different laboratories. The results agree with existing models, reflect differences in mechanisms of charge transport and rectification, and are predictive in cases where experimental limitations preclude more sophisticated modeling. We also synthesized a series of conjugated molecular wires, in which embedded dipoles are varied systematically and at both molecule–electrode interfaces. The resulting current–voltage characteristics vary in nonintuitive ways that are not captured by existing models, but which produce trends using our simple model, providing insights that are otherwise difficult or impossible to explain. The utility of our model is its demonstrative generalizability, which is why simple observables like tunneling decay coefficients remain so widely used in molecular electronics despite the existence of much more sophisticated models. Our model is complementary, giving insights into molecule–electrode coupling across series of molecules that can guide synthetic chemists in the design of new molecular motifs, particularly in the context of devices comprising large-area molecular junctions.

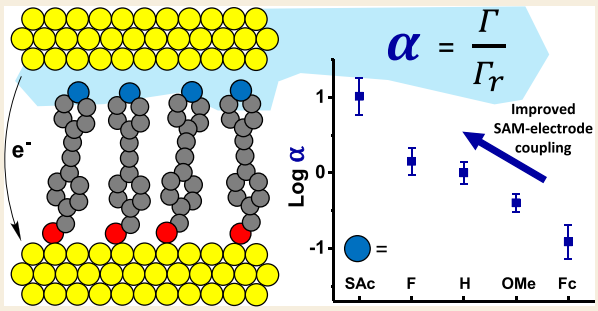

KEYWORDS: *single-level model, EGaIn, self-assembled monolayers, interface, molecular electronics*

INTRODUCTION

Molecular tunneling junctions can comprise single molecules or ensembles of molecules. While the former can be modeled atomistically to gain fundamental insights into charge transport, the same features that make the latter promising for technological applications make them difficult to model.[1−4] Large-area molecular junctions usually incorporate self-assembled monolayers (SAMs) that are dynamic, supramolecular ensembles, which make them prohibitively computationally expensive on their own, let alone sandwiched between two electrodes.[5−8] Moreover, many aspects of the SAM–electrode interface that vary with the composition of the electrode are still not well-understood.[5,8−10] Collective effects in SAMs can strongly affect tunneling charge transport, such as when surface-confined dipoles give rise to electric fields that shift the work functions (ϕ) of the electrodes[6,7,11] or alter the electrostatic profile of the SAM itself.[12] While some of these phenomena have been investigated theoretically and measured experimentally in SAMs,[7,11] it is not completely clear how and to what extent these collective properties (in)directly influence charge-transport properties in a large-area molecular junction. For example, using eutectic gallium–indium (EGaIn) electrodes, Whitesides et al. demonstrated that changing the anchoring group (i.e., the interfacial dipole at the non-EGaIn electrode), inserting dipoles with varying orientation in the middle of a junction, or functionalizing with different end-groups at the SAM//EGaIn interface did not significantly affect the charge-transport properties.[13−16] Only fluorination of the molecules at the SAM//EGaIn interface was shown to lower the current density (without altering the transport mechanism), but it was ascribed to worse wetting of the EGaIn electrode, leading to smaller contact areas.[17] The effects of polar groups at the SAM//EGaIn interface are, however, still a matter of debate; while some researchers report similar findings,[18,19] others found charge transport to be either more or less sensitive to the nature of the surface dipoles.[20,21]

As a result, the understanding of the effects of molecular dipoles in junctions is still insufficient to enable deterministic molecular design.[19,22] This limitation remains true even for

Received: September 14, 2021
Revised: December 20, 2021
Accepted: December 22, 2021
Published: January 12, 2022

https://doi.org/10.1021/acsphyschemau.1c00029
ACS Phys. Chem Au 2022, 2, 179–190

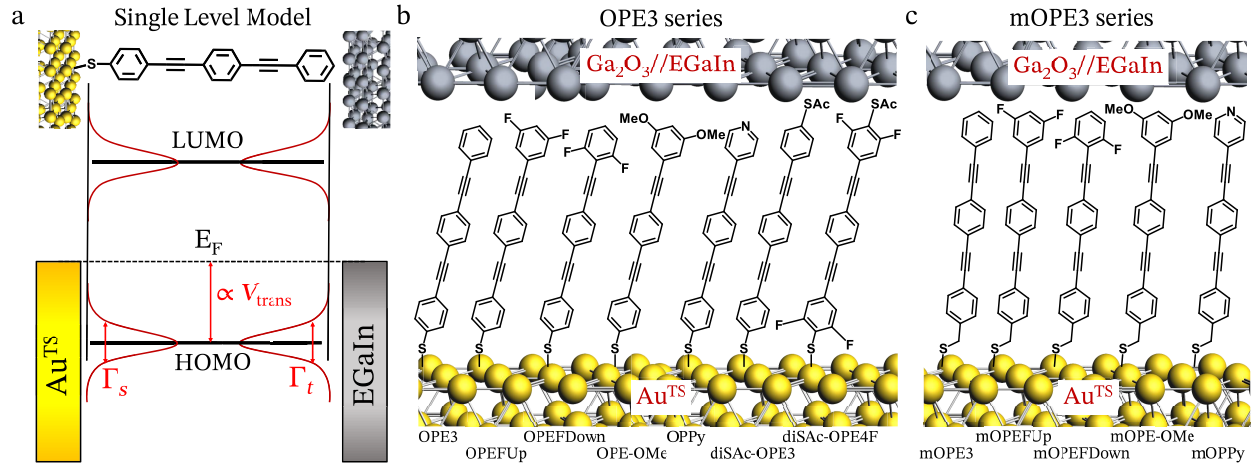

Figure 1. (a) Schematic of the single-level model used for this study showing the energy offset that is proportional to V_{trans} and the coupling parameters to the tip and the substrate as Γ_s and Γ_t, respectively. The SLM only considers the contribution of the most dominant molecular orbital, which can either be the highest occupied (HOMO) or the lowest unoccupied molecular orbital (LUMO). (b) The functionalized OPE3 molecular wires investigated individually in this study with thiol as the anchoring group; parent OPE3 is taken as a reference molecule, shown together in a large-area molecular junction with EGaIn as the top electrode and Au^{TS} as the bottom electrode. (c) Functionalized mOPE3 molecular wires with a methylene bridge connecting the conjugated core to the thiol anchoring group; parent mOPE3 was taken as a reference. The abbreviations used in this study for all these wires are included at the bottom of the figure. Structures of a few other molecules of these two series are shown in Table S2 in the Supporting Information.

simple saturated molecules, where the lack of accessible molecular states lends itself to relatively straightforward modeling through a rectangular tunneling barrier.[16,23,24] SAMs comprising conjugated molecules were shown to be more sensitive to collective properties of SAMs, such as dipoles.[19,25−27] These collective effects make a conjugated molecular wire even more difficult to model.

The limiting factor in developing predictive models that can translate molecular structure to collective effects (and the electrical properties of a device) is the lack of precision of the inputs. While it is possible to select defect-free regions of a SAM and estimate the number of molecules in a junction with a well-defined probe tip, it is not possible to construct a (proto)device using a probe tip as a top contact. Instead, device-relevant platforms rely on the SAM to define the smallest dimension of the device, by applying a conformal top contact to a defined area of a SAM. This approach produces static, functional electrical devices, but it includes defects, grain boundaries, and other idiosyncrasies of supramolecular ensembles of molecules bound to a surface. We propose that the first step toward solving these problems is to apply simple, retrospective models to large numbers of junctions comprising a wide variety of molecular ensembles measured in many different laboratories to surface trends that are otherwise occluded by noisy data and the paucity of generalizable models.

This paper introduces a single-level model (SLM; Figure 1a) to describe the relative coupling at the SAM//EGaIn interface in large-area molecular junctions. We are using two parameters that are easily obtained from the standard current versus voltage (I/V) data: low-bias current and transition voltage. We show that the SLM applies to various series of molecules that share a backbone composition. Although this method does not provide direct insights into energy offsets, it captures details of the interfacial environment between the SAM and the top electrode (EGaIn) that are currently absent from existing models and explains nonintuitive trends in conjugated molecular wires. The purpose of this SLM is not to probe the minutia of tunneling charge-transport mechanisms or validate underlying theories. It is to provide a simple way to extract a meaningful parameter across series of molecules that can aid in the deterministic design and synthesis of molecules (much like the tunneling decay coefficient β is often used as a benchmark in the design of experimental platforms for constructing molecular junctions). Moreover, it requires only data that one can readily extract from the $J-V$ electrical characterization of the junctions, without the need for further experiments or even fits to $J-V$ curves. This simplicity allows researchers to directly compare data between different sets of molecules and experimental techniques as well as across laboratories. Existing studies are mostly limited to small sets of molecules, making it difficult to test models and extract generalizable design rules. And, while there are models that can provide mechanistic insights based on experimental input parameters,[28−32] the parameters are either nontrivial (compared to I/V traces) to determine[33,35] or specific to a given experimental platform.[36−41] As a result, it is difficult to construct general design rules from comparisons across different studies. We chose to focus this study on large-area junctions, because they are the most technologically relevant among all ME platforms, albeit being the most difficult to model.

To begin with, we demonstrate the utility of the SLM on conjugated molecular wires by analyzing a series of molecules bearing oligo(phenylene-ethynylene) (OPE) cores. We systematically vary the identities and positions of polar groups within the junction synthetically, e.g., thioacetate (diSAc-OPE3), 3,5-difluoro (OPEFUp), 2,6-difluoro (OPEFDown), 3,5-dimethoxy (OPE-OMe), and pyridino (OPPy). We are able to separate the effects of the two different electrode interfaces by modifying the anchoring group: the thioacetate (−SAc) anchoring group is either directly conjugated to the OPE, e.g., OPE3, or separated by a methylene bridge ($-CH_2-$SAc), e.g., mOPE3. This simple synthetic modification in the anchoring group provides us with an easy handle on a number of important parameters: (i) the angle between the molecular

https://doi.org/10.1021/acsphyschemau.1c00029
ACS Phys. Chem Au 2022, 2, 179−190

dipoles and the metal surface; (ii) molecular packing; and (iii) the extent of the coupling of the conjugated π-orbitals with the bottom electrode (see Figure 1b).[42,43] These synthetic modifications capture the useful properties of OPEs that are the reason they are widely studied in molecular junctions: they can be functionalized without affecting the planarity of the π-conjugated backbone, the frontier orbitals of which dominate charge transport, while their polarizability provides a handle for perturbation through the inclusion of functional groups. We also demonstrate the utility of the SLM on saturated molecules by analyzing published data on junctions that rectify current via different mechanisms, but that are modulated by interactions at the SAM//EGaIn interface.[22,44−46]

We measured the charge-transport properties of SAMs of all newly synthesized compounds in large-area Au^{TS}/SAM//EGaIn molecular junctions (where "/" and "//" denote covalent and van der Waals interactions, respectively, and Au^{TS} indicates atomically flat, template-stripped Au surfaces[47]). We followed the measurements protocol established in our previous work,[48] which is also briefly described in the Supporting Information in section 4. By analyzing both the magnitudes and line shapes of current density (J) versus voltage (V) plots across this diverse series, we were able to quantify the influence of the dipoles at the interface numerically and differentiate the dipolar and interfacial contributions to the overall charge-transport characteristics. We also analyzed the normalized differential conductance (NDC)[49] plots and extracted the transition voltages (V_{trans})[50] as described in the Supporting Information in section 4. We also performed simulations and density functional theory (DFT) calculations on gas-phase optimized geometries of all the molecules to study their electronic properties with and without the presence of metal electrodes. These simulations offer further insights into the experimental results and support the validity of our SLM model.

RESULTS AND DISCUSSION

Single-Level Model

Single-level models are analytical tools developed from the Landauer formalism, in which charge transport is dominated by a single molecular level (HOMO in the case of OPEs) to the extent that contributions from other levels can be ignored. To quantify the role of the interface in tunneling characteristics in large-area junctions with EGaIn top contacts, we modified the SLM developed by Bâldea and Frisbie for junctions with conducting-probe atomic force microscopy (CPAFM) top contacts.[9,36,51] Their SLM expresses tunneling current $I(V)$ and current density $J(V)$ as

$$J(V) = \frac{I(V)}{A} = \frac{4NG_0}{A}\frac{V\Gamma^2}{3V_{trans}^2 - V^2} \quad (1)$$

where G_0 is the conductance quantum ($2e^2\,h^{-1} = 77.48\ \mu S$), N is the number of molecules in the junction, A is the area of the junction, and V_{trans} is the transition voltage. The latter is an empirical term derived from experimental current density versus voltage (J/V) or I/V curves and is related to the energy offset between the electrodes and the molecular orbital closest to the Fermi level (E_f).[36,52−55] Γ is the interfacial coupling parameter between the SAM and the electrodes and, because of the asymmetric contacts, is the geometric average of the coupling parameters corresponding to the top contact Γ_t and the bottom substrate Γ_s. In our case, for every molecular series, the binding geometry of the anchoring group to the bottom substrate is the same, and hence, the coupling parameter Γ_s can be considered constant for a molecular series. A more detailed explanation of the SLM is provided in the Supporting Information. Estimating N and Γ is rather straightforward for CPAFM junctions,[9] because the density of a SAM can be determined experimentally, and the area of the junction is well-defined for the rigid CPAFM top contact, which is small enough to exclude the defects (e.g., pinholes and grain boundaries) that are present in SAMs. Large-area contacts such as EGaIn add a number of complexities: (i) the unknown (and variable) chemical nature of the contact;[56−58] (ii) the difference between the actual and measured (geometrical) contact area;[59] (iii) the unavoidable inclusion of defects; and (iv) the diverse conditions under which various large-area contacts are applied. These complexities also tend to produce smaller values of V_{trans} (particularly for EGaIn) than CPAFM, which narrows the bias window over which eq 1 can be applied.

The current/above-mentioned version of the SLM requires certain modifications to extract quantitative trends of the SAM//EGaIn interfacial coupling parameter (α), relative to a reference SAM. For the conjugated series studied in this work (Figure 1b,c), we used SAMs of mOPE3 and OPE3 as references for the SAMs with and without methylene spacers at the thiol anchoring group, respectively. Even though it is true that this is an "extra" measurement, a reference (or control) SAM is almost always measured anyway in ME studies, and usually, it comprises molecules as structurally similar as possible to those that are the main focus of the studies. Thus, using this modified approach, we obtain the ratio $J_r(V)$ by dividing the J of a SAM by that of the reference (J^{ref}) in the low-bias regime and use eq 1 to obtain

$$\lim_{V\to 0} J_r(V) = \lim_{V\to 0}\frac{J(V)}{J^{ref}(V)} = \frac{\Gamma_t}{\Gamma_t^{ref}}\cdot\left(\frac{V_{trans}^{ref}}{V_{trans}}\right)^2 \quad (2)$$

which can be rearranged to extract the relative SAM//EGaIn surface interaction parameter, $\alpha = \Gamma_t/\Gamma_t^{ref}$ as a function of the low-bias conductance ratio ($\lim_{V\to 0} J_r(V)$) and V_{trans}

$$\alpha = \frac{\Gamma_t}{\Gamma_t^{ref}} = \left(\frac{V_{trans}}{V_{trans}^{ref}}\right)^2\cdot\lim_{V\to 0} J_r(V) \quad (3)$$

The transition voltage (V_{trans}) identifies the voltage at which the current−voltage characteristics of a nonresonant tunneling junction change from a linear regime (found at low bias) to a hyperlinear one. It is usually calculated as the minimum in the Fowler−Nordheim plot or the maximum of $|V^2/J|$ obtained from the measured J/V curves.[38,60,61] We determined V_{trans} using normalized differential conductance plots, NDC = $(dJ/dV)^*(V/J)$, by following the procedure described by Vilan et al.[43,49] Using this method, V_{trans} is determined from the voltage at which NDC = 2, and it can also be extrapolated from any point in the curve more readily than using Fowler−Nordheim plots. This method is mathematically equivalent to those reported earlier, and it allows for a more precise estimation of V_{trans} when it falls close or outside of the investigated bias window.[22,23,25,44,52−54,62] Moreover, NDC plots can give information about the transport mechanisms, because a "bowl-shaped" curvature (with a minimum value of 1 for V = 0) correlates well to nonresonant transport. (This feature is particularly useful in the case of special cases and unusual

https://doi.org/10.1021/acsphyschemau.1c00029
ACS Phys. Chem Au 2022, 2, 179−190

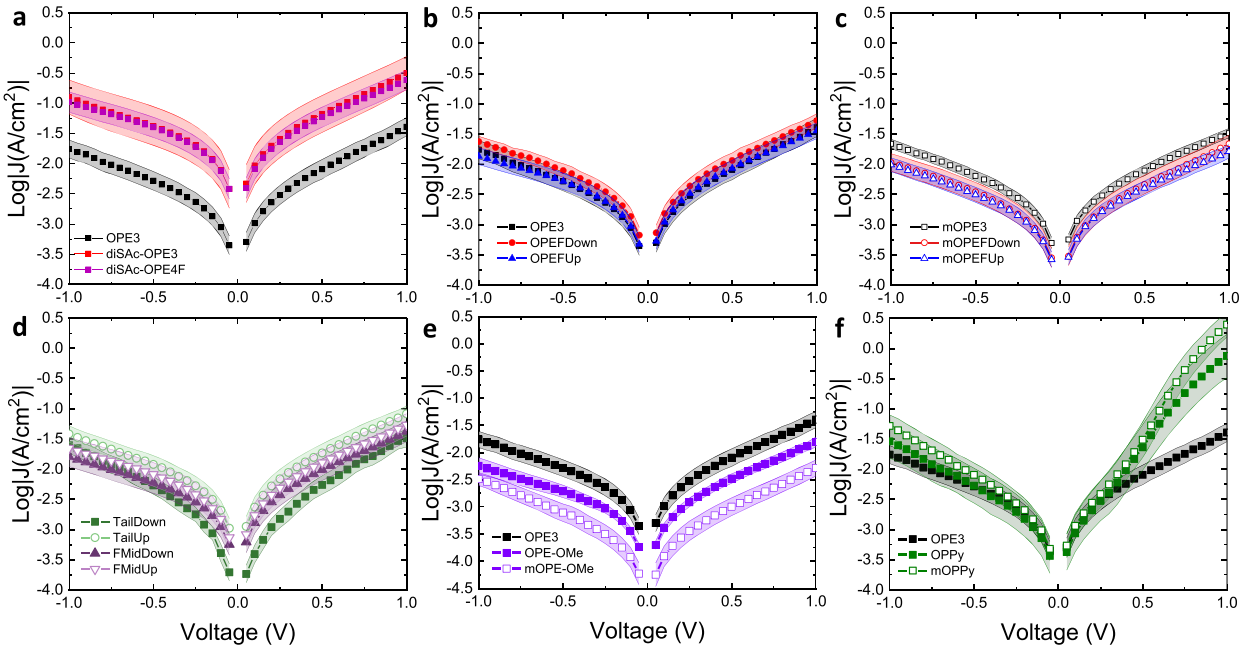

Figure 2. Plots of log|*J*| vs *V* for Au^{TS}/SAM//Ga_2O_3/EGaIn junctions comprising the following compounds: (a) OPE3, diSAc-OPE3, and diSAc-OPE4F, (b) OPEFDown and OPEFUp compared to OPE3, (c) mOPEFDown and mOPEFUp compared to mOPE3, (d) fluorinated analogues of OPE3: TailDown, TailUp, FMidUp, and FMidDown of the OPEF series, (e) OPE-OMe and mOPE-OMe compared to OPE3, and (f) OPPy and mOPPy compared to OPE3. Error bars represent 95% confidence intervals. See Figure 1 and Table S2 for molecular structures.

phenomena such as quantum interference.[63]) A detailed derivation and explanation of eq 3 can be found in the Supporting Information together with examples of the application of this approach on other SAMs. Here, via α, we use our modified SLM to compare the interface characteristics of EGaIn junctions comprising different molecules and, consequently, separate effects arising from inherent molecular properties from interfacial phenomena. We chose α to express the ratio of the two Γ parameters that can determined from *J*/*V* data for large-area junctions; compared to the Γ parameter that describes single-molecule and few-molecule junctions, α is less well-defined, because it captures the intrinsic complexity and heterogeneity of the totality of molecule−electrode interactions over a relatively large area. Values of $\alpha > 1$ and $\alpha < 1$ indicate stronger and weaker interactions at the SAM// electrode interface compared to the reference SAM. Thus, even though our SLM does not directly capture energy offsets, it directly addresses the relative influence of electronic effects from interfacial effects, which, across a sufficiently large set of data, provides direct information about how and why synthetic modifications translate into the electrical characteristics of large-area molecular junctions.

Conjugated Backbones

Thioacetate-Terminated Wires. Molecules with symmetric thioacetate termini (diSAc-) are common in SAM-based molecular electronics, because they offer simpler synthetic procedures compared to their asymmetric analogues.[48,64] They can be studied directly in single-molecule junctions for comparison, and the acetate groups are easily cleaved *in situ* during the formation of a SAM or a single-molecule junction.[64] One side effect of using symmetric thioacetates is that the deprotection strategy needed to afford a high-quality SAM leaves them largely intact at the ambient interface.[65] For the reasons discussed above, we do not expect free thiols to form covalent bonds to EGaIn, but the dipole moments of the thioacetate groups may facilitate coupling, which would be reflected in the SLM. To better understand the subtle differences in the *J*/*V* curves, we calculated the asymmetry $\chi = \frac{J(V_+)}{J(V_-)}$ (Figure S9), and the normalized differential conductance, NDC = $\left(\frac{dJ}{dV}\cdot\frac{V}{J}\right)$ (Figure S10). Information on the tunneling transport that is not readily apparent in the *J*/*V* curves can be extracted from NDC plots instead.[43,49] Analysis of the NDC can give one information about the energy level alignment in the junction and the transport mechanism. Large-area EGaIn molecular junctions usually give rise to a small asymmetry, which is often ascribed to the different electrodes/contacts involved[26] or Stark effects.[22,45,66]

The *J*/*V* data for diSAc-OPE3 are shown in Figure 2a together with those for OPE3 (which lack the -SAc group at the EGaIn interface).[48] It is evident that SAMs of the former are more conductive across the entire bias window. According to DFT calculations, the addition of a thioacetate group does not significantly shift the orbital energies with respect to OPE3. A deeper inspection of the *J*/*V* curves revealed that χ and V_{trans} are extremely similar for the two compounds, in agreement with the DFT calculations. The most plausible explanation for the difference in conductance is the SAc//EGaIn interaction itself, highlighting the ability of polar functional groups to affect the magnitude of the current without affecting the electronic structure vis-à-vis DFT calculations and V_{trans} (i.e., in the gas phase or via empirical observations in assembled junctions). We previously showed that junctions comprising SAMs of diSAc-OPE3 yielded larger injection currents (J_0) compared to their OPE analogues.[48] We ascribed this difference to the more favorable interactions between diSAc-OPE3 and the EGaIn electrode, which increases the number of molecules in contact, increasing the effective area of the junction rather than affecting the tunneling charge transport

https://doi.org/10.1021/acsphyschemau.1c00029
ACS Phys. Chem Au 2022, 2, 179−190

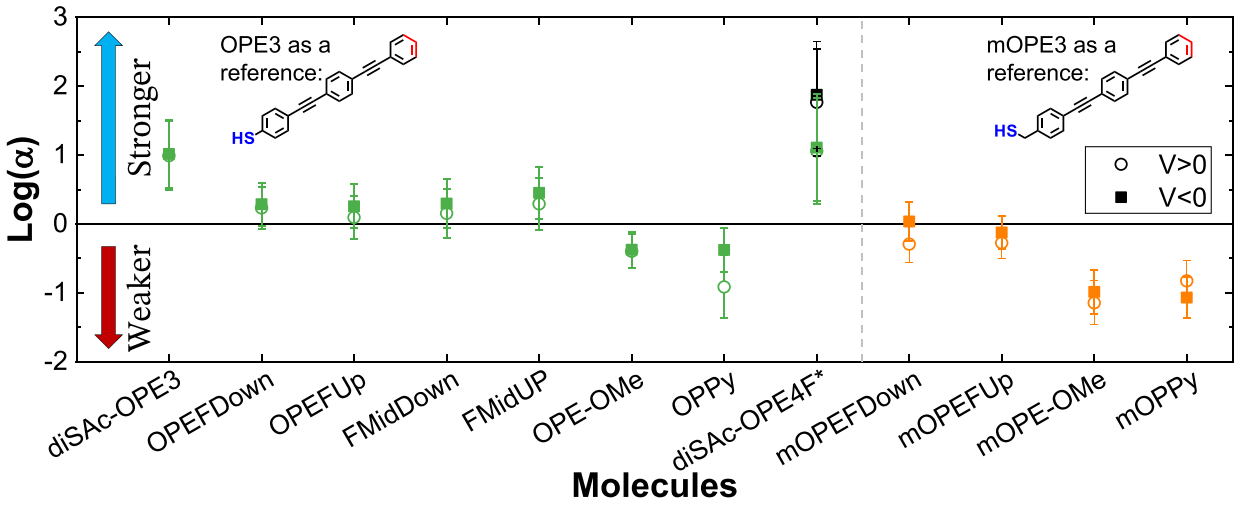

Figure 3. Semilog plot of the predicted surface interaction parameter (α) using SLM for the SAM//EGaIn interface for the OPE series (green data points) with a thiol anchoring group with OPE3 as the reference (*for diSAc-OPE4F, green and black data points represent log(α) with OPE3 and TailDown—see Supporting Information for structure—as references, respectively). The orange data points represent log(α) for the mOPE series with a methylene spacer to the thiol anchoring group and, therefore, mOPE3 as the reference molecule. A horizontal line at $Y = 0$ is drawn to highlight the trends. The values of α are provided in Table S2 in the Supporting Information.

Table 1. Summary of DFT-Calculated Energies of the Gas-Phase HOMO, LUMO, and Band Gap in eV as Well as Dipole Moments from DFT in Debye (along the Length of the Molecular Wire)[a]

compounds	HOMO	LUMO	band gap	dipole	nonshorting junctions (%)	V^{+}_{trans}	V^{-}_{trans}
OPE3	−5.63	−2.09	3.54	0.52	93[48]	0.65	0.8
OPEFUp	−5.82	−2.35	3.47	−2.55	96	0.70	−1.11
OPEFDown	−5.72	−2.23	3.48	1.03	73	0.69	−0.98
OPE-OMe	−5.57	−2.00	3.57	3.53	83	0.64	−0.88
OPPy	−5.84	−2.38	3.46	−3.40	88	0.25	−0.60
diSAc-OPE3	−5.56	−2.11	3.45	0.00	92[48]	0.68	−0.92
diSAc-OPE4F	−5.96	−2.52	3.44	0.00	82	0.65	−1.09
mOPE3	−5.75	−2.13	3.61	0.02	52	0.78	−0.89
mOPEFUp	−5.98	−2.38	3.59	−3.03	31	0.75	−1.00
mOPEFDown	−5.86	−2.27	3.59	0.54	72	0.72	−1.16
mOPE-OMe	−5.68	−2.05	3.63	3.01	96	0.66	−0.83
mOPPy	−5.98	−2.37	3.60	−4.14	88	0.29	−0.55

[a]The last three columns summarize the experimental yield of working junctions and V_{trans} (V) at positive and negative bias for Au^{TS}/SAM//EGaIn tunneling junctions for the molecules shown in Figure 1.

directly.[48,59] However, the SLM reveals that the α parameter for diSAc-OPE3 is an order of magnitude higher than that of OPE3, suggesting that the larger values of J_0 were, in fact, due to higher rates of tunneling charge transport. This result agrees with the SLM analysis by Frisbie and co-workers showing that oligophenylenedithiols couple stronger than oligophenylene-monothiols.[61]

Changing the length of the OPE chains (e.g., diSAc-OPE2 and diSAc-OPE4, relative to OPE2 and OPE4, respectively), does not alter α significantly (Figure S14). Moreover, α values are comparable among other series of molecules with similar length and diSAc- termination (see Figure S14 and Table S2). These findings suggest that the influence of the diSAc-anchoring group is consistent across different series of compounds and that it specifically affects the SAM//EGaIn interface.

Difluorinated Wires. The introduction of fluorines to the backbone (OPEF) affects the electronic properties of the OPE wires (by lowering the HOMO and the LUMO). Fluorines also introduce a strong dipole to the molecule itself and (particularly when installed at a terminus) molecule−electrode interface(s). Figure 2 summarizes the J/V properties of EGaIn junctions comprising OPE wires with systematically varied F-substituents. There is no apparent correlation between the magnitude of J and the position or magnitude of the molecular dipoles compared to OPE3; the SAMs gave statistically indistinguishable results for magnitude and line shape of J ($\chi \approx 0.35$ at 1 V, see the Supporting Information). The interaction with the top electrode is slightly stronger, with $\alpha \approx 1.4$, which is similar to the respective values for the isomers bearing the fluorines on the middle ring (see Figure 3 and Table S2). Likewise, the addition of fluorines to diSAc-OPE3 (e.g., diSAc-OPE4F) yielded slightly higher values of α compared to the parent diSAc-OPE3. These results suggest that fluorination of the phenyl rings of OPEs slightly increases the strength of coupling with the top electrode. For diSAc-OPE4F, we computed α with respect to OPE3 and TailDown (see the Supporting Information for structure) as references in Figure 3. diSAc-OPE4F with four fluorine substituents ortho to the sulfur anchor show stronger coupling to the top electrode compared to the difluorinated molecules. diSAc-OPE4F also shows a stronger interaction compared to the TailDown

https://doi.org/10.1021/acsphyschemau.1c00029
ACS Phys. Chem Au 2022, 2, 179−190

reference molecule, which has only two F-substituents ortho to the bottom sulfur anchor and is a monothiol molecule. These results highlight that while the trends in α from our analysis are neatly preserved, the correct choice of reference molecule is paramount.

The only significant difference that we were able to discern between fluorinated OPEs and their unsubstituted analogues concerns V_{trans}. As shown in Table 1, the introduction of fluorine atoms increases the magnitudes of $|V^{-}_{trans}|$ and $|V^{+}_{trans}|$. While previous studies have shown that the shift in vacuum level induced by the collective effects of dipoles leads to a correlation between the direction of the dipoles and V_{trans},[26,67] this correlation is not apparent for OPE3 derivatives. Instead, the shift in V_{trans} is correlated to lower HOMO energies, suggesting that the SLM is valid and that transport is dominated by the HOMO. Since this shift is apparently in V_{trans}, it should suppress conductance contrary to our observation in Figure 2; our approach reveals that this effect is exactly offset by the increase in α.

The effect of dipoles on the electrical characteristic of large-area junctions is often explained by invoking molecular packing and dipole alignment in SAMs.[12,27] The missing correlation in the OPEF series could indicate that the SAMs are too sparse (i.e., tilted) to provide sufficient cooperative interaction between the dipoles to shift the vacuum level, which could be related to the tendency of fluorinated molecules to weaken dispersion forces. Analogous to the depressed boiling and melting points of fluorinated hydrocarbons, SAMs of OPEF may be more liquid-like and less densely packed than SAMs of OPE. And since collective effects become measurable only when a high degree of cooperative interaction is found in the SAM,[68] electronic effects (lower HOMO, higher α) are dominant in SAMs of OPEF.

Methoxy-Terminated Wires. While the electronic properties of the OPE-OMe wires are similar to those of the parent OPE wires, the interfacial chemistry in SAMs is strikingly different. Methyl groups of the methoxy units are oriented outward as a result of the steric constraints, pointing them toward the EGaIn electrode and forming an interface that more closely resembles that of an alkane. This interfacial arrangement can affect overall transport by increasing the effective width of the junction, (which manifests in a large value of β) and altering the interaction between SAM and EGaIn (which manifests in $\alpha \neq 1$).[69] This is also true for the diSAc-OPE3 wires as they introduce polar groups to the interface and increase the molecular length. In addition to the interfacial effects, methoxy groups exhibit very large dipoles, which can influence transport in all of the ways discussed above.

We found J for these systems to be smaller than that of the unsubstituted wires (Figure 2), while χ and V_{trans} are notably similar, despite the significant difference in molecular dipoles (Table 1). These observations are exactly the opposite of what we found for OPEF; methoxy substituents raise the HOMO energy, but instead of increasing, J decreases. The lack of a commensurate change in V_{trans} suggests that a weaker interaction is offsetting the influence of the HOMO, and indeed, the SLM reveals $\alpha < 1$ (Figure 3).

Pyridino-Terminated Wires. We further investigated the role of dipoles at the interface by using a structural analogue of OPE3 but bearing a pyridine ring at the SAM//EGaIn interface (OPPy). These compounds introduce a highly polar and a possible coordinating group to the EGaIn interface, have a very strong dipole (pointing in the opposite direction than the OPE-OMe wires), and have low HOMO and LUMO values, similar to OPEF but greater in magnitude. It has been shown previously using rigorous (HR)XPS, NEXAFS, STM, and IR characterization that SAMs of conjugated molecules with pyridyl and thiol terminal groups orient with pyridines facing upward with the thiol acting as the dominant anchoring group.[70−73] In our previous study too, we have also utilized SAMs of pyridine-terminated conjugated molecular wires.[25] The shapes of the J/V curves for SAMs of OPPy are notably different from those of the other OPE wires (Figure 2); at low and negative bias, J is comparable for OPE3 and OPPy, but at high, positive bias they differ by about 1.5 orders of magnitude. Similar asymmetry is also present in the J/V curves for SAMs of mOPPy. Log χ does not scale linearly with bias but shows an almost sigmoidal trend, with onsets around 0.2 and 0.4 V for OPPy and mOPPy, respectively. The peculiar behavior of these systems is also highlighted in the NDC plots (see Supporting Information), which, while still being bowl-shaped around 0 V, is characterized by a peak at positive bias with a maximum around 0.55 V. The structural properties and chemical bonding of freshly prepared OPPy and mOPPy SAMs were measured by X-ray photoelectron spectroscopy (XPS) in UHV conditions. The intensity ratio of chemisorbed (161.9−162.0 eV) and physisorbed (163.6−163.8 eV) sulfur suggest that 70% of both the SAMs were grafted covalently to the gold surface, whereas 30% of the SAMs were physically bonded to the Au surface. The presence of the C=O peak indicates the presence of the protecting acetyl group or environmental impurities in mOPPy SAMs. The N 1s in the both SAMs has a prominent pyridinic nitrogen indicating that 90% of SAMs were chemically preserved on the gold surface, whereas the second peak at the high binding energy peak could correspond to the pyridine molecule forming hydrogen bonds with adsorbed water molecules.

The unusual behavior of OPPy could be a result of either the low-lying LUMO or the interaction between the pyridyl groups and the EGaIn electrode. The characteristic feature in the NDC plot can be ascribed to the presence of the accessible unoccupied level that comes into resonance with E_f at positive bias.[43,49] This bias-induced effect is also evident from the transmission spectra (see Supporting Information), which show a new feature at $E - E_f = 1$ eV. We have noticed a similar behavior in our previous study about COOH-terminated alkanethiolates showing rectification.[22] We suspect that both COOH and pyridino SAMs have similar rectifying mechanisms, and therefore, similar α values as shown in Figure 3. The rectification behavior of the pyridino SAMs will be further investigated in a follow-up study.

Methylenated OPE3 SAMs. The addition of an extra $-CH_2-$ between the conjugated backbone and the S−metal bond in the SAM (mOPE series) significantly affects the packing and the nature of the molecules in the SAM in three major ways: (i) the tilt angle of the conjugated part in SAMs of mOPE molecules is larger (i.e., the molecular axis is closer to the surface normal);[74] (ii) the benzylic $-CH_2-$ reduces the coupling between the molecules and the substrate by partially separating the electron density of the molecular orbitals from that of the metal states;[42,75] and (iii) the presence of the methylene also slightly affects the electronic characteristics of the compounds, lowering the HOMO by about 0.1 eV. mOPE3 and its analogues therefore represent a good platform to extend the scope of the SLM and the α parameter even

https://doi.org/10.1021/acsphyschemau.1c00029
ACS Phys. Chem Au 2022, 2, 179−190

further by altering the SAM/Au interface. For this series, values of α are referenced to mOPE3.

The addition of the methylene unit at the anchoring group does not significantly influence the magnitude of J (Figure 2). It was previously reported that one methylene group is not enough to completely decouple the conjugated part of a molecule from the bottom electrode.[42,43] Calculated transmission probabilities for OPE3 and mOPE3 support this finding (see Supporting Information). Nonetheless, the introduction of $-CH_2-$ at the SAM/Au interface alters the symmetry of the junction: the maximum value of χ = 2.2 for OPE3 but only 1.5 for mOPE3 at 1 V (see Supporting Information, Figure S9). Thus, whatever degree of decoupling is affected by $-CH_2-$ renders the SAM/Au interface more similar to the EGaIn//SAM interface.[76] This trend is consistent throughout the mOPE3 series.

Interestingly, some features appear in SAMs of mOPEF that are not present in mOPE or in their nonmethylenated analogues, OPEF. For instance, J decreases, as was also observed for fluorinated mercapto-alkanes[17] and halogen-terminated polyphenylenes.[19,77] The values of V_{trans} are similar to those found for the OPEF wires, suggesting that the electronic effects of the substituents do not differ significantly. The SLM is also consistent in that α is slightly smaller for mOPEF than for OPEF, reflecting the partial decoupling of the Au/SAM interface. However, recently, Asyuda et al. studied the effects of mixed SAMs with different terminations comprising (4-methyl)phenyl and (4-trifluoromethyl)phenyl groups on charge transport in Au/SAM//EGaIn junctions as shown in Figure 4a.[67] We applied our simplified SLM on their

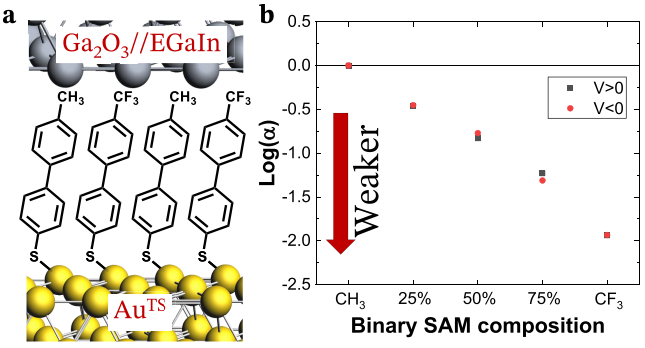

Figure 4. (a) Schematic of a binary SAM containing CH_3-BPT/CF_3-BPT molecules in different ratios taken from ref 77. The CF_3 group induces the dipole moment away from thiol group, in contrast to the CH_3 group whose dipole moment is pointed toward the thiol group. (b) Semilog plot of the predicted surface interaction parameter (α) with an increasing portion of CF_3-BPT in the solution from which the binary SAMs were prepared. The predicted α value shows a reducing trend with increased CF_3 groups on the SAM//EGaIn interface.

data using the pure SAMs of CH_3-BPT as the reference SAM and computing the relative α parameter for the SAMs with an increasing concentration of CF_3-BPT molecules on the surface in the binary SAMs. Figure 4b shows that the $-CF_3$ moiety at the interface weakens the interaction with the electrode—unlike in OPEF when fluorines are directly attached to the phenyl rings—lowering the α about 2 orders of magnitude compared to $-CH_3$. This application of our model to a published data set obtained from another research group clearly demonstrates the ease with which it can be applied to elucidate the interfacial coupling of SAMs with top EGaIn electrode.

Introducing $-CH_2-$ units to the OPE-OMe and OPPy wires resulted in comparable yet enhanced trends; mOPE-OMe is even less conductive than OPE-OMe, and χ is larger for mOPPy than OPPy. However, α is significantly smaller for both mOPPy and mOPE-OMe than their fully conjugated analogues. This difference may be due to packing and the aforementioned weaker intermolecular interactions in OPEF, but elucidating these details experimentally is beyond the scope of this paper.

DFT Modeling. To support the J/V measurements, we simulated transmission spectra of all the OPE and mOPE molecular wires (see section 6 of the Supporting Information). We report the gas-phase frontier energy levels and dipole moments in Figure S19. Transmission simulations, shown in Figure S20, were performed on model systems comprising single molecules between Au metal clusters and do not account for interface effects with EGaIn. Nevertheless, they provide qualitative support for several observations: (i) (m)OPEOMe is the least conductive; (ii) (m)OPE3 is similar in conductance to (m)OPEFUp and (m)OPEFDown, as the transmission features are just shifted in energy due to electron withdrawing F groups, which would explain different asymmetries in J/V curves; (iii) diSAc-OPE3 and diSAc-OPE4F are more conductive than OPE3; and (iv) the unique asymmetry in $J-V$ curves of (m)OPPy is also reflected in emergence of a new transmission peak at ~1 eV above E_f.

Aliphatic Backbones

COOH Rectifier. As discussed above, α is not simply a measure of changes at the molecule//electrode interface even though formally it is a ratio of values of Γ. However, in SAMs with aliphatic backbones, trends in α should map on to changes in the head groups, because the backbones are not polarizable, and the electronic structure will, therefore, be minimally impacted by the identity of the functional groups at the molecule/electrode interfaces.

We previously demonstrated that SAMs of alkanethiolates terminated with carboxylic acids rectify current in their hydrated state using EGaIn, CPAFM, and reduced graphene oxide as top electrodes.[22] When dehydrated, these SAMs no longer rectify current. This observation, explained via lowering of the LUMO level due to the Stark effect, is hypothesized to occur due to the weak coupling between the COOH terminal group and the top electrode. This hypothesis is supported by the observation that strong R-COOH//EGaIn interactions would have displaced weakly bound water molecules from the SAM interface, such that the hydration state of the SAM would have no influence on electrical properties. If that hypothesis is correct, the SLM should show weak coupling between COOH and the top electrode.

Figure 5 compares SAMs terminated with COOH in both the hydrated (rectifying) and dehydrated (nonrectifying) states with a SAM comprising alkanethiolates of the same length (denoted C16SH for hexadecanethiol) as a reference. The values of α, which are tabulated in Table S2 and also shown in Figure 5, were computed according to eq 3. Not only is COOH much more weakly coupled to EGaIn than CH_3, but α also differs in the hydrated and dehydrated states. This finding is counterintuitive, as one would expect SAMs with high surface free energies (i.e., more polar or polarizable head groups) to have a stronger interaction with the electrodes. But

https://doi.org/10.1021/acsphyschemau.1c00029
ACS Phys. Chem Au 2022, 2, 179−190

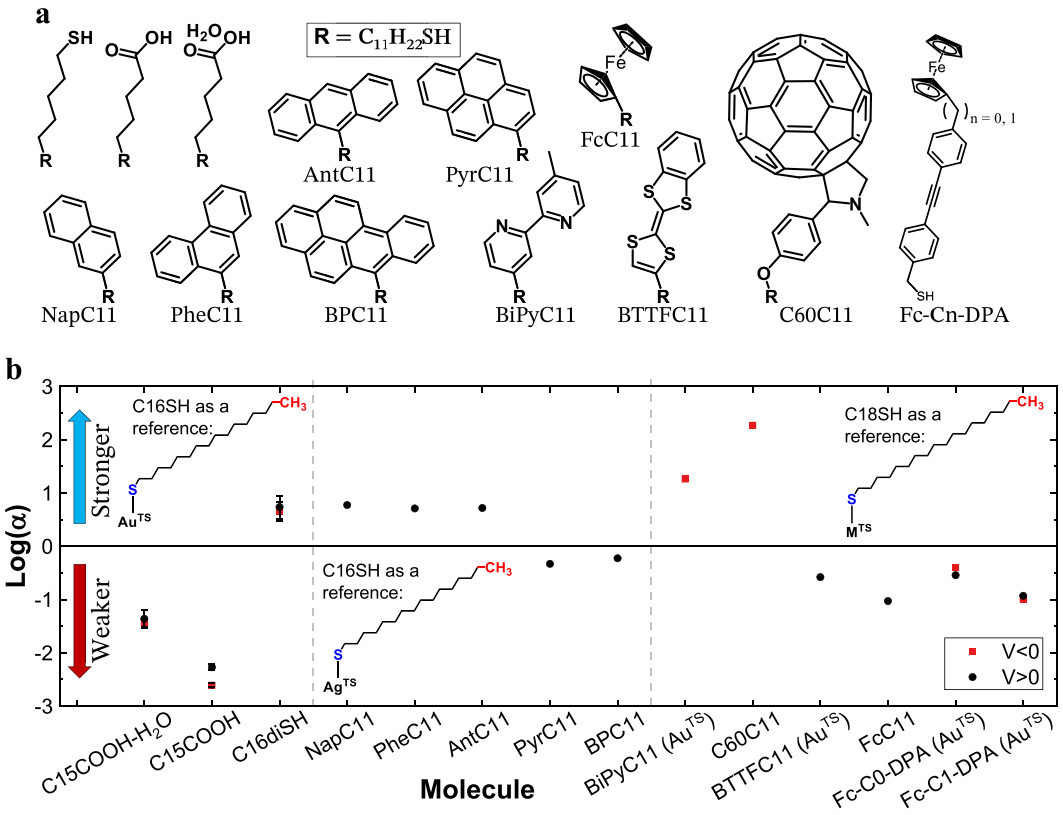

Figure 5. (a) Molecular structures with an aliphatic tail and headgroups as thiol (C16diSH), carboxylic acid (C15COOH), and hydrated carboxylic acid (C15COOH-H_2O) taken from ref 22.; naphthyl (NapC11), phenanthrenyl (PheC11), anthracenyl (AntC11), pyrenyl (PyrC11), benzo[a]pyrenyl (BPC11), and bipyridyl (BiPyC11) from refs 44 and 45; and tetrathiafulvalene (BTTF),[78] ferrocene (FcC11), fullerene (C60C11),[46] and ferrocene-diphenylacetylene (Fc-C*n*-DPA for n = 0, 1).[34] The **R** group represents the undecanethiol ($C_{11}H_{22}SH$). (b) Semilog plot of the predicted surface interaction parameter (α) using SLM for the SAM//EGaIn interface for (left panel) alkylcarboxylic acid in rectifying and nonrectifying states[22] and hexadecanedithiol, using C16SH as the reference molecule; (middle panel) all the molecules in the arene series on Ag^{TS} substrates using the data from Yoon group, Korea University; and (right panel) miscellaneous rectifiers with C18SH reference measured on Ag^{TS}, except for BiPyC11, BTTFC11, and Fc-C*n*-DPA, which were measured on Au^{TS}, and hence, a C18SH measured on Au^{TS} was used as a reference. Note that, for several rectifying molecules, the SLM was only applied at the nonrectifying bias polarity due to ambiguities in the extraction of V_{trans} at rectifying bias polarities.

it supports the hypothesis that rectification is driven by the Stark effect. Further, SLM predicts stronger coupling for hexadecanedithiol (C16diSH) compared to the reference monothiol, in agreement with the higher α for diSAc-OPE3 than OPE3 and also with the work published by Frisbie and co-workers on CPAFM junctions.[8]

Miscellaneous Rectifiers. Our simplified model does not, a priori, account for rectification; however, it also demonstrably does not fail when applied to systems that exhibit rectification (i.e., asymmetric J/V curves). We propose that because the coupling between the SAM and the EGaIn electrode plays a critical role in most rectification mechanisms observed in large-area junctions, the underlying physical process manifests in α. Yoon et al. reported various degrees of rectification from a series of arene-terminated, aliphatic SAMs caused by the Stark effect (Figure 5a).[45] In the case of COOH-terminated SAMs, the hydration state of the SAM shifted the LUMO close enough to E_f for the Stark effect to induce rectification, while Yoon et al. modulated the HOMO and LUMO synthetically, by investigating arenes with different bond topologies. The authors used photoelectron spectroscopy to show that for NapC11, PheC11, and AntC11, the LUMO was localized near the EGaIn interface, while for PyrC11 and BPC11, the HOMO was in proximity of EGaIn.[45] Figure 5 shows that log α is the same for NapC11, PheC11, and AntC11, meaning that the SAM//EGaIn coupling does not differ significantly. Interestingly, $\chi \approx 1$ for all three of these SAMs (reported in ref 45); however, $\chi \approx 150$ for PyrC11 and $\chi \approx 50$ for BPC11 and log $\alpha \approx -0.3$ for both, meaning that a weak interaction correlates to a large, Stark-effect-induced rectification. As described above, weak coupling is also correlated to rectification for COOH-terminated SAMs. All of these SAMs are hypothesized to rectify by the Stark effect, in which the energies of molecular orbitals shift in an applied electric field. Since strongly coupled molecular orbitals would tend to follow E_f, weak coupling would facilitate the stark effect induced rectification. As shown by Nijhuis et al., BTTFC11, consisting of a tetrathiafulvalene core, does not rectify on Ag^{TS} substrates but does rectify on Au^{TS} at positive bias. This observation is ascribed to the involvement of HOMO, which does not track E_f and comes in resonance at positive bias such that charge transfer occurs between BTTF and the S−Au interface.[78] This rectification mechanism is the same as that proposed by van Dyck and Ratner, who showed that rectification can occur in asymmetrical molecules where the HOMO and LUMO are located on either terminus of the molecule and follow the electric field gradient in the junction, because they come into resonance for one bias polarity and out of resonance for the other.[79] This mechanism is similar to PyrC11 and BPC11, as discussed above, and is consistent with

https://doi.org/10.1021/acsphyschemau.1c00029
ACS Phys. Chem Au 2022, 2, 179−190

the weak coupling of BTTFC11 on Au^{TS} revealed by log α. In recent studies, Yoon et al. reported rectification mechanism in pure and mixed SAMs of BiPyC11, charge-transport transitions from the normal to inverted Marcus regime.[80,81] The authors demonstrated that rectification occurs following the aforementioned model proposed by van Dyck and Ratner[79] due to the strong Fermi level pinning of the LUMO on the BiPy moiety and the HOMO on the thiol anchor to EGaIn and Au^{TS} (Figure S17c). We assert that this mechanism results from the strong coupling at the top interface revealed by the large α value in Figure 5. While a large value of α is too crude to capture the interplay between Fermi level pinning, the Stark effect, and the Marcus effect, it has the practical advantage of actually being measurable across these series of disparate models; trends in α, therefore, can act as a guide for deeper theoretical investigation. Further, C60C11 is proposed to rectify via the same mechanism as BiPyC11,[46] but variable-temperature measurements are (currently) prohibited by low yields in stabilized junctions (which are necessary at low temperatures). The similarity in α is evidence of a shared mechanism that is otherwise precluded by experimental limitations. Indeed, the two SAMs in Figure 5 that show large values of α, BiPyC11 and C60C11, are hypothesized to rectify through strongly coupled, unoccupied molecular orbitals that track E_f.[44,46]

Lastly, we applied our SLM on molecules with ferrocene head-groups attached to a diphenyleneacetylene moiety (Fc-C*n*-DPA; n = 0, 1) studied by Yuan et al.[34] Fc-C1-DPA rectifies via the same mechanism as FcC11 (Figure S17a),[82] while Fc-C0-DPA follows a different mechanism in a Marcus-inverted regime (Figure S17) where an unoccupied orbital localized on the DPA moiety gates the chemical potential of the occupied orbital localized on the Fc moiety (Figure S17b). As shown in Figure 5, the Fc-C1-DPA molecule shows weak coupling similar to FcC11, because both of them are HOMO-mediated rectifiers, while Fc-C0-DPA shows stronger coupling, which is necessary for the gating phenomenon. The rigorous and complex experiments required to elucidate that phenomenon do not apply to all systems—e.g., Fc-C0-DPA forms particularly robust SAMs, and comparisons to electrostatic gates require thiols at both interfaces—yet, our simple SLM tracks the underlying electrode−molecule coupling, further underscoring its potential for identifying areas of potential interest for more rigorous investigation by enabling surveys and comparisons of α across large series of compounds and experimental platforms.

CONCLUSIONS

Models to describe tunneling charge transport through molecular junctions must be able to produce trends across large series of molecules in order to be useful for synthetic chemists in the deterministic design of new molecules and experiments. Although sophisticated DFT calculations can often reproduce nonintuitive observations about trends in conductance, their sophistication makes it difficult to draw straightforward conclusions that are relevant at the level of molecular design. We have demonstrated a simple SLM that readily produced trends of a molecule/electrode coupling parameter across more than 40 large-area junctions comprising a wide variety of (SAMs of) molecules. The input parameters, which are low-bias current density (J for $V \rightarrow 0$) and transition voltages, are readily and reproducibly measured, do not require to perform additional targeted experiments, and can be easily extracted from published $J-V$ data, which allowed us to apply our SLM model on the data from several different laboratories.

We examined data from aliphatic and conjugated molecules with varied functional groups at the electrode interfaces and the backbones. For conjugated molecules, the SLM explained J/V characteristics that were nonintuitive; conductance could be reproduced using DFT but not explained. The trends produced by the SLM intuitively captured the decoupling effect of the insertion of a $-CH_2-$ between the thiol anchor and the conjugated backbone. They also revealed that the chemical nature of the functional group strongly affects the interaction between the SAM and the EGaIn electrode and that the lack of substituent effects is, at least in part, due to stronger pinning (due to molecule−electrode coupling) offsetting shifts in molecular orbital energies. Finally, we applied the simplified SLM to junctions measured in other laboratories that rectify current through the Stark effect, intramolecular gating, or by molecular orbitals tracking E_f, demonstrating the usefulness of the model in systems with complex $J-V$ relationships. Moreover, trends produced by the SLM predicted mechanisms of rectification that otherwise can not be determined experimentally. Further, the coupling parameter that the simplified SLM produces is referenced to a benchmark junction, meaning it is only useful for examining relative trends. However, we believe its simplicity and the fact that it does not rely on fitting J/V curves will make it particularly useful to chemists and to researchers working to extract a useful, device-relevant function from large-area molecular junctions. To the best of our knowledge, this is the only single-level model that has been applied on such a wide range of SAMs measured by different users in different laboratories and produced consistent results.

ASSOCIATED CONTENT

Supporting Information

The Supporting Information is available free of charge at https://pubs.acs.org/doi/10.1021/acsphyschemau.1c00029.

Details of synthesis and chemical characterizations; SAM fabrication procedure and SAM and substrate characterization using XPS and AFM; details of $J-V$ measurements using the EGaIn top electrode; formulation and adaptation of the single-level model; details of DFT simulations and geometrical coordinates (PDF)

AUTHOR INFORMATION

Corresponding Author

Ryan C. Chiechi − *Stratingh Institute for Chemistry, University of Groningen, 9747 AG Groningen, The Netherlands;* Present Address: Department of Chemistry, North Carolina State University, Raleigh, North Carolina 27695-8204, United States. (R.C.C.); orcid.org/0000-0002-0895-2095; Email: rchiech@ncsu.edu

Authors

Marco Carlotti − *Stratingh Institute for Chemistry, University of Groningen, 9747 AG Groningen, The Netherlands;* Present Address: Italian Institute of Technology, Center for MicroBioRobotics, Viale Rinaldo Piagio 34, 56025, Pontedera, Italy. (M.C.); orcid.org/0000-0001-8086-7613

Saurabh Soni − *Stratingh Institute for Chemistry, University of Groningen, 9747 AG Groningen, The Netherlands;* Present

https://doi.org/10.1021/acsphyschemau.1c00029
ACS Phys. Chem Au 2022, 2, 179−190

Address: Hybrid Materials for Optoelectronics Group, Department of Molecules and Materials, Faculty of Science and Technology, University of Twente, P.O. Box 217, 7500 AE Enschede, The Netherlands. (S.S.); orcid.org/0000-0002-8159-9128

Andrii Kovalchuk − *Stratingh Institute for Chemistry, University of Groningen, 9747 AG Groningen, The Netherlands*

Sumit Kumar − *Electrical Engineering Division, Department of Engineering, University of Cambridge, Cambridge CB3 0FA, U.K.*

Stephan Hofmann − *Electrical Engineering Division, Department of Engineering, University of Cambridge, Cambridge CB3 0FA, U.K.;* orcid.org/0000-0001-6375-1459

Complete contact information is available at: https://pubs.acs.org/10.1021/acsphyschemau.1c00029

Author Contributions

¶M.C. and S.S. contributed equally to this paper.

Notes

The authors declare no competing financial interest.

■ ACKNOWLEDGMENTS

R.C.C., M.C., and A.K. acknowledge the European Research Council for the ERC Starting Grant 335473 (MOLECSYNCON). S.S. acknowledges the Zernike Institute for Advanced Materials. We thank the Center for Information Technology of the University of Groningen for their support and for providing access to the Peregrine high performance computing cluster. M.C. gratefully acknowledges partial support from the European Unions Horizon 2020 research and innovation programme under the Marie Skodowska-Curie grant agreement 885881 (MP3). S.K. and S.H. acknowledge funding from EPSRC (EP/T001038/1). We thank Prof. Hyo Jae Yoon, Prof. Michael Zharnikov, and Prof. Christian Nijhuis and their group members for useful discussions and sharing their data.

■ REFERENCES

(1) Xiang, D.; Wang, X.; Jia, C.; Lee, T.; Guo, X. Molecular-Scale Electronics: From Concept to Function. *Chem. Rev.* **2016**, *116*, 4318−4440.

(2) Chen, B.; Xu, K. Single Molecule-Based Electronic Devices: A Review. *Nano* **2019**, *14*, 1930007.

(3) Vuillaume, D. Molecular Electronics: From Single-Molecule to Large-Area Devices. *ChemPlusChem.* **2019**, *84*, 1215−1221.

(4) Karuppannan, S. K.; Neoh, E. H. L.; Vilan, A.; Nijhuis, C. A. Protective Layers Based on Carbon Paint to Yield High-Quality Large-Area Molecular Junctions With Low Contact Resistance. *J. Am. Chem. Soc.* **2020**, *142*, 3513−3524.

(5) Heimel, G.; Rissner, F.; Zojer, E. Modeling the Electronic Properties of Pi-Conjugated Self-Assembled Monolayers. *Adv. Mater.* **2010**, *22*, 2494−2513.

(6) Kretz, B.; Egger, D. A.; Zojer, E. A Toolbox for Controlling the Energetics and Localization of Electronic States in Self-Assembled Organic Monolayers. *Adv. Sci.* **2015**, *2*, 1400016.

(7) Cabarcos, O. M.; Schuster, S.; Hehn, I.; Zhang, P. P.; Maitani, M. M.; Sullivan, N.; Giguère, J.-B.; Morin, J.-F.; Weiss, P. S.; Zojer, E.; Zharnikov, M.; Allara, D. L. Effects of Embedded Dipole Layers on Electrostatic Properties of Alkanethiolate Self-Assembled Monolayers. *J. Phys. Chem. C* **2017**, *121*, 15815−15830.

(8) Xie, Z.; Bâldea, I.; Frisbie, C. D. Energy Level Alignment in Molecular Tunnel Junctions by Transport and Spectroscopy: Self-Consistency for the Case of Alkyl Thiols and Dithiols on Ag, Au, and Pt Electrodes. *J. Am. Chem. Soc.* **2019**, *141*, 18182−18192.

(9) Xie, Z.; Bâldea, I.; Oram, S.; Smith, C. E.; Frisbie, C. D. Effect of Heteroatom Substitution on Transport in Alkanedithiol-Based Molecular Tunnel Junctions: Evidence for Universal Behavior. *ACS Nano* **2017**, *11*, 569−578.

(10) Bâldea, I. Protocol for Disentangling the Thermally Activated Contribution to the Tunneling-Assisted Charge Transport. Analytical Results and Experimental Relevance. *Phys. Chem. Chem. Phys.* **2017**, *19*, 11759−11770.

(11) Alloway, D. M.; Hofmann, M.; Smith, D. L.; Gruhn, N. E.; Graham, A. L.; Colorado, R.; Wysocki, V. H.; Lee, T. R.; Lee, P. A.; Armstrong, N. R. Interface Dipoles Arising From Self-Assembled Monolayers on Gold: UV-Photoemission Studies of Alkanethiols and Partially Fluorinated Alkanethiols. *J. Phys. Chem. B* **2003**, *107*, 11690−11699.

(12) Abu-Husein, T.; Schuster, S.; Egger, D. A.; Kind, M.; Santowski, T.; Wiesner, A.; Chiechi, R. C.; Zojer, E.; Terfort, A.; Zharnikov, M. The Effects of Embedded Dipoles in Aromatic Self-Assembled Monolayers. *Adv. Funct. Mater.* **2015**, *25*, 3943−3957.

(13) Bowers, C. M.; Liao, K.-C.; Zaba, T.; Rappoport, D.; Baghbanzadeh, M.; Breiten, B.; Krzykawska, A.; Cyganik, P.; Whitesides, G. M. Characterizing the Metal-Sam Interface in Tunneling Junctions. *ACS Nano* **2015**, *9*, 1471−1477.

(14) Yoon, H. J.; Shapiro, N. D.; Park, K. M.; Thuo, M. M.; Soh, S.; Whitesides, G. M. The Rate of Charge Tunneling Through Self-Assembled Monolayers Is Insensitive to Many Functional Group Substitutions. *Angew. Chem., Int. Ed.* **2012**, *51*, 4658−4661.

(15) Yoon, H. J.; Bowers, C. M.; Baghbanzadeh, M.; Whitesides, G. M. The Rate of Charge Tunneling Is Insensitive to Polar Terminal Groups in Self-Assembled Monolayers in $Ag^{TS}S(CH_2)_nM(CH_2)_mT//Ga_2O_3$/EGaIn Junctions. *J. Am. Chem. Soc.* **2014**, *136*, 16−19.

(16) Baghbanzadeh, M.; Pieters, P. F.; Yuan, L.; Collison, D.; Whitesides, G. M. The Rate of Charge Tunneling in EGaIn Junctions Is Not Sensitive to Halogen Substituents at the Self-Assembled Monolayer//Ga_2O_3 Interface. *ACS Nano* **2018**, *12*, 10221−10230.

(17) Liao, K.-C.; Bowers, C. M.; Yoon, H. J.; Whitesides, G. M. Fluorination, and Tunneling Across Molecular Junctions. *J. Am. Chem. Soc.* **2015**, *137*, 3852−3858.

(18) Kong, G. D.; Kim, M.; Jang, H.-J.; Liao, K.-C.; Yoon, H. J. Influence of Halogen Substitutions on Rates of Charge Tunneling Across SAM-based Large-Area Junctions. *Phys. Chem. Chem. Phys.* **2015**, *17*, 13804−13807.

(19) Chen, X.; Annadata, H. V.; Kretz, B.; Zharnikov, M.; Chi, X.; Yu, X.; Egger, D. A.; Nijhuis, C. A. Interplay of Collective Electrostatic Effects and Level Alignment Dictates the Tunneling Rates Across Halogenated Aromatic Monolayer Junctions. *J. Phys. Chem. Lett.* **2019**, *10*, 4142−4147.

(20) Wang, D.; Fracasso, D.; Nurbawono, A.; Annadata, H. V.; Sangeeth, C. S. S.; Yuan, L.; Nijhuis, C. A. Tuning the Tunneling Rate and Dielectric Response of SAM-Based Junctions via a Single Polarizable Atom. *Adv. Mater.* **2015**, *27*, 6689−6695.

(21) Bruce, R. C.; You, L.; Förster, A.; Pookpanratana, S.; Pomerenk, O.; Lee, H. J.; Marquez, M. D.; Ghanbaripour, R.; Zenasni, O.; Lee, T. R.; Hacker, C. A. Contrasting Transport and Electrostatic Properties of Selectively Fluorinated Alkanethiol Monolayers With Embedded Dipoles. *J. Phys. Chem. C* **2018**, *122*, 4881−4890.

(22) Ai, Y.; Kovalchuk, A.; Qiu, X.; Zhang, Y.; Kumar, S.; Wang, X.; Kühnel, M.; Nørgaard, K.; Chiechi, R. C. In-Place Modulation of Rectification in Tunneling Junctions Comprising Self-Assembled Monolayers. *Nano Lett.* **2018**, *18*, 7552−7559.

(23) Nijhuis, C. A.; Reus, W. F.; Whitesides, G. M. Mechanism of Rectification in Tunneling Junctions Based on Molecules With Asymmetric Potential Drops. *J. Am. Chem. Soc.* **2010**, *132*, 18386−18401.

(24) Kong, G. D.; Kim, M.; Cho, S. J.; Yoon, H. J. Gradients of Rectification: Tuning Molecular Electronic Devices by the Controlled

Use of Different-Sized Diluents in Heterogeneous Self-Assembled Monolayers. *Angew. Chem., Int. Ed.* **2016**, *55*, 10307−10311.
(25) Fracasso, D.; Muglali, M. I.; Rohwerder, M.; Terfort, A.; Chiechi, R. C. Influence of an Atom in EGaIn/Ga2O3 Tunneling Junctions Comprising Self-Assembled Monolayers. *J. Phys. Chem. C* **2013**, *117*, 11367−11376.
(26) Kovalchuk, A.; Abu-Husein, T.; Fracasso, D.; Egger, D. A.; Zojer, E.; Zharnikov, M.; Terfort, A.; Chiechi, R. C. Transition Voltages Respond to Synthetic Reorientation of Embedded Dipoles in Self-Assembled Monolayers. *Chem. Sci.* **2016**, *7*, 781−787.
(27) Kovalchuk, A.; Egger, D. A.; Abu-Husein, T.; Zojer, E.; Terfort, A.; Chiechi, R. C. Dipole-Induced Asymmetric Conduction in Tunneling Junctions Comprising Self-Assembled Monolayers. *RSC Adv.* **2016**, *6*, 69479−69483.
(28) Migliore, A.; Schiff, P.; Nitzan, A. On the Relationship Between Molecular State and Single Electron Pictures in Simple Electrochemical Junctions. *Phys. Chem. Chem. Phys.* **2012**, *14*, 13746.
(29) Kim, H.; Segal, D. Controlling Charge Transport Mechanisms in Molecular Junctions: Distilling Thermally Induced Hopping From Coherent-Resonant Conduction. *J. Chem. Phys.* **2017**, *146*, 164702.
(30) Liu, J.; Segal, D. Generalized Input-Output Method to Quantum Transport Junctions. II. Applications. *Phys. Rev. B* **2020**, *101*, 155407.
(31) Jauho, A.-P.; Wingreen, N. S.; Meir, Y. Time-Dependent Transport in Interacting and Noninteracting Resonant-Tunneling Systems. *Phys. Rev. B* **1994**, *50*, 5528−5544.
(32) Liu, J.; Segal, D. Generalized Input-Output Method to Quantum Transport Junctions. I. General Formulation. *Phys. Rev. B* **2020**, *101*, 155406.
(33) Garrigues, A. R.; Yuan, L.; Wang, L.; Mucciolo, E. R.; Thompon, D.; del Barco, E.; Nijhuis, C. A. A Single-Level Tunnel Model to Account for Electrical Transport through Single Molecule- and Self-Assembled Monolayer-based Junctions. *Sci. Rep.* **2016**, *6*, 26517.
(34) Yuan, L.; Wang, L.; Garrigues, A. R.; Jiang, L.; Annadata, H. V.; Anguera Antonana, M.; Barco, E.; Nijhuis, C. A. Transition From Direct to Inverted Charge Transport Marcus Regions in Molecular Junctions via Molecular Orbital Gating. *Nat. Nanotechnol.* **2018**, *13*, 322−329.
(35) Garrigues, A. R.; Yuan, L.; Wang, L.; Singh, S.; del Barco, E.; Nijhuis, C. A. Temperature Dependent Charge Transport Across Tunnel Junctions of Single-Molecules and Self-Assembled Monolayers: A Comparative Study. *Dalton Trans.* **2016**, *45*, 17153−17159.
(36) Bâldea, I. Ambipolar Transition Voltage Spectroscopy: Analytical Results and Experimental Agreement. *Phys. Rev. B* **2012**, *85*, 035442.
(37) Xie, Z.; Bâldea, I.; Frisbie, C. D. Why One Can Expect Large Rectification in Molecular Junctions Based on Alkane Monothiols and Why Rectification Is So Modest. *Chem. Sci.* **2018**, *9*, 4456−4467.
(38) Smith, C. E.; Xie, Z.; Bâldea, I.; Frisbie, C. D. Work Function and Temperature Dependence of Electron Tunneling Through an N-Type Perylene Diimide Molecular Junction With Isocyanide Surface Linkers. *Nanoscale* **2018**, *10*, 964−975.
(39) Song, X.; Yu, X.; Hu, W. Model Study on the Ideal Current−Voltage Characteristics and Rectification Performance of a Molecular Rectifier Under Single-Level-Based Tunneling and Hopping Transport. *J. Phys. Chem. C* **2020**, *124*, 24408−24419.
(40) Song, X.; Han, B.; Yu, X.; Hu, W. The Analysis of Charge Transport Mechanism in Molecular Junctions Based on Current-Voltage Characteristics. *Chem. Phys.* **2020**, *528*, 110514.
(41) Valianti, S.; Cuevas, J.-C.; Skourtis, S. S. Charge-Transport Mechanisms in Azurin-Based Monolayer Junctions. *J. Phys. Chem. C* **2019**, *123*, 5907−5922.
(42) Yuan, L.; Nerngchamnong, N.; Cao, L.; Hamoudi, H.; del Barco, E.; Roemer, M.; Sriramula, R. K.; Thompson, D.; Nijhuis, C. A. Controlling the Direction of Rectification in a Molecular Diode. *Nat. Commun.* **2015**, *6*, 6324.
(43) Zhang, Y.; Soni, S.; Krijger, T. L.; Gordiichuk, P.; Qiu, X.; Ye, G.; Jonkman, H. T.; Herrmann, A.; Zojer, K.; Zojer, E.; Chiechi, R. C. Tunneling Probability Increases With Distance in Junctions Comprising Self-Assembled Monolayers of Oligothiophenes. *J. Am. Chem. Soc.* **2018**, *140*, 15048−15055.
(44) Yoon, H. J.; Liao, K.-C.; Lockett, M. R.; Kwok, S. W.; Baghbanzadeh, M.; Whitesides, G. M. Rectification in Tunneling Junctions: 2,2′-Bipyridyl-Terminated N-Alkanethiolates. *J. Am. Chem. Soc.* **2014**, *136*, 17155−17162.
(45) Cho, S. J.; Kong, G. D.; Park, S.; Park, J.; Byeon, S. E.; Kim, T.; Yoon, H. J. Molecularly Controlled Stark Effect Induces Significant Rectification in Polycyclic-Aromatic-Hydrocarbon-Terminated N-Alkanethiolates. *Nano Lett.* **2019**, *19*, 545−553.
(46) Qiu, L.; Zhang, Y.; Krijger, T. L.; Qiu, X.; van't Hof, P.; Hummelen, J. C.; Chiechi, R. C. Rectification of Current Responds to Incorporation of Fullerenes Into Mixed-Monolayers of Alkanethiolates in Tunneling Junctions. *Chem. Sci.* **2017**, *8*, 2365−2372.
(47) Weiss, E. A.; Kaufman, G. K.; Kriebel, J. K.; Li, Z.; Schalek, R.; Whitesides, G. M. Si/SiO_2-templated Formation of Ultraflat Metal Surfaces on Glass, Polymer, and Solder Supports: Their Use as Substrates for Self-Assembled Monolayers. *Langmuir* **2007**, *23*, 9686−9694.
(48) Carlotti, M.; Degen, M.; Zhang, Y.; Chiechi, R. C. Pronounced Environmental Effects on Injection Currents in EGaIn Tunneling Junctions Comprising Self-Assembled Monolayers. *J. Phys. Chem. C* **2016**, *120*, 20437−20445.
(49) Vilan, A. Revealing Tunnelling Details by Normalized Differential Conductance Analysis of Transport Across Molecular Junctions. *Phys. Chem. Chem. Phys.* **2017**, *19*, 27166−27172.
(50) Beebe, J. M.; Kim, B.; Gadzuk, J. W.; Frisbie, C. D.; Kushmerick, J. G. Transition from Direct Tunneling to Field Emission in Metal-Molecule-Metal Junctions. *Phys. Rev. Lett.* **2006**, *97*, 026801.
(51) Xie, Z.; Bâldea, I.; Smith, C. E.; Wu, Y.; Frisbie, C. D. Experimental and Theoretical Analysis of Nanotransport in Oligophenylene Dithiol Junctions as a Function of Molecular Length and Contact Work Function. *ACS Nano* **2015**, *9*, 8022−8036.
(52) Beebe, J. M.; Kim, B.; Frisbie, C. D.; Kushmerick, J. G. Measuring Relative Barrier Heights in Molecular Electronic Junctions With Transition Voltage Spectroscopy. *ACS Nano* **2008**, *2*, 827−832.
(53) Huisman, E. H.; Guédon, C. M.; van Wees, B. J.; van der Molen, S. J. Interpretation of Transition Voltage Spectroscopy. *Nano Lett.* **2009**, *9*, 3909−3913.
(54) Guo, S.; Hihath, J.; Díez-Pérez, I.; Tao, N. Measurement and Statistical Analysis of Single-Molecule Current-Voltage Characteristics, Transition Voltage Spectroscopy, and Tunneling Barrier Height. *J. Am. Chem. Soc.* **2011**, *133*, 19189−19197.
(55) Zhang, Y.; Ye, G.; Soni, S.; Qiu, X.; Krijger, T. L.; Jonkman, H. T.; Carlotti, M.; Sauter, E.; Zharnikov, M.; Chiechi, R. C. Controlling Destructive Quantum Interference in Tunneling Junctions Comprising Self-Assembled Monolayers via Bond Topology and Functional Groups. *Chem. Sci.* **2018**, *9*, 4414−4423.
(56) Weiss, E. A.; Chiechi, R. C.; Kaufman, G. K.; Kriebel, J. K.; Li, Z.; Duati, M.; Rampi, M. A.; Whitesides, G. M. Influence of Defects on the Electrical Characteristics of Mercury-Drop Junctions: Self-Assembled Monolayers of N-Alkanethiolates on Rough and Smooth Silver. *J. Am. Chem. Soc.* **2007**, *129*, 4336−4349.
(57) Carlotti, M.; Soni, S.; Kumar, S.; Ai, Y.; Sauter, E.; Zharnikov, M.; Chiechi, R. C. Two-Terminal Molecular Memory Through Reversible Switching of Quantum Interference Features in Tunneling Junctions. *Angew. Chem., Int. Ed.* **2018**, *57*, 15681−15685.
(58) Pourhossein, P.; Vijayaraghavan, R. K.; Meskers, S. C. J.; Chiechi, R. C. Optical Modulation of Nano-Gap Tunnelling Junctions Comprising Self-Assembled Monolayers of Hemicyanine Dyes. *Nat. Commun.* **2016**, *7*, 11749.
(59) Simeone, F. C.; Yoon, H. J.; Thuo, M. M.; Barber, J. R.; Smith, B.; Whitesides, G. M. Defining the Value of Injection Current and Effective Electrical Contact Area for EGaIn-Based Molecular Tunneling Junctions. *J. Am. Chem. Soc.* **2013**, *135*, 18131−18144.
(60) Metzger, R. M. Quo vadis, unimolecular electronics? *Nanoscale* **2018**, *10*, 10316−10332.

https://doi.org/10.1021/acsphyschemau.1c00029
ACS Phys. Chem Au 2022, 2, 179−190

(61) Xie, Z.; Bâldea, I.; Frisbie, C. D. Determination of Energy-Level Alignment in Molecular Tunnel Junctions by Transport and Spectroscopy: Self-Consistency for the Case of Oligophenylene Thiols and Dithiols on Ag, Au, and Pt Electrodes. *J. Am. Chem. Soc.* **2019**, *141*, 3670−3681.
(62) Lefèvre, X.; Moggia, F.; Segut, O.; Lin, Y.-P.; Ksari, Y.; Delafosse, G.; Smaali, K.; Guérin, D.; Derycke, V.; Vuillaume, D.; Lenfant, S.; Patrone, L.; Jousselme, B. Influence of Molecular Organization on the Electrical Characteristics of Pi-Conjugated Self-Assembled Monolayers. *J. Phys. Chem. C* **2015**, *119*, 5703−5713.
(63) Carlotti, M.; Soni, S.; Qiu, X.; Sauter, E.; Zharnikov, M.; Chiechi, R. C. Systematic Experimental Study of Quantum Interference Effects in Anthraquinoid Molecular Wires. *Nanoscale Advances* **2019**, *1*, 2018−2028.
(64) Kaliginedi, V.; Moreno-García, P.; Valkenier, H.; Hong, W.; García-Suárez, V. M.; Buiter, P.; Otten, J. L. H.; Hummelen, J. C.; Lambert, C. J.; Wandlowski, T. Correlations Between Molecular Structure and Single-Junction Conductance: A Case Study With Oligo(phenylene-Ethynylene)-Type Wires. *J. Am. Chem. Soc.* **2012**, *134*, 5262−5275.
(65) Valkenier, H.; Huisman, E. H.; van Hal, P. A.; de Leeuw, D. M.; Chiechi, R. C.; Hummelen, J. C. Formation of High-Quality Self-Assembled Monolayers of Conjugated Dithiols on Gold: Base Matters. *J. Am. Chem. Soc.* **2011**, *133*, 4930−4939.
(66) Li, Y.; Zolotavin, P.; Doak, P.; Kronik, L.; Neaton, J. B.; Natelson, D. Interplay of Bias-Driven Charging and the Vibrational Stark Effect in Molecular Junctions. *Nano Lett.* **2016**, *16*, 1104−1109.
(67) Asyuda, A.; Wan, X.; Zharnikov, M. Binary Aromatic Self-Assembled Monolayers: Electrostatic Properties and Charge Tunneling Rates Across the Molecular Framework. *Phys. Chem. Chem. Phys.* **2020**, *22*, 10957−10967.
(68) Dubi; Yonatan. Transport Through Self-Assembled Monolayer Molecular Junctions: Role of in-Plane Dephasing. *J. Phys. Chem. C* **2014**, *118*, 21119−21127.
(69) Liao, K.-C.; Hsu, L.-Y.; Bowers, C. M.; Rabitz, H.; Whitesides, G. M. Molecular Series-Tunneling Junctions. *J. Am. Chem. Soc.* **2015**, *137*, 5948−5954.
(70) Silien, C.; Buck, M.; Goretzki, G.; Lahaye, D.; Champness, N. R.; Weidner, T.; Zharnikov, M. Self-Assembly of a Pyridine-Terminated Thiol Monolayer on Au(111). *Langmuir* **2009**, *25*, 959−967.
(71) Liu, J.; Schüpbach, B.; Bashir, A.; Shekhah, O.; Nefedov, A.; Kind, M.; Terfort, A.; Wöll, C. Structural characterization of self-assembled monolayers of pyridine-terminated thiolates on gold. *Phys. Chem. Chem. Phys.* **2010**, *12*, 4459.
(72) Wächter, T.; Weinhardt, L.; Terfort, A.; Zharnikov, M. Pyridine as a Resonantly Addressable Group to Study Electron-Transfer Dynamics in Self-Assembled Monolayers. *J. Phys. Chem. C* **2018**, *122*, 12534−12544.
(73) Sauter, E.; Yildirim, C.; Terfort, A.; Zharnikov, M. Adjustment of the Work Function of Pyridine and Pyrimidine Substituted Aromatic Self-Assembled Monolayers by Electron Irradiation. *J. Phys. Chem. C* **2017**, *121*, 12834−12841.
(74) Love, J. C.; Estroff, L. a.; Kriebel, J. K.; Nuzzo, R. G.; Whitesides, G. M. Self-Assembled Monolayers of Thiolates on Metals as a Form of Nanotechnology. *Chem. Rev.* **2005**, *105*, 1103−1170.
(75) Neaton, J. B.; Hybertsen, M. S.; Louie, S. G. Renormalization of Molecular Electronic Levels at Metal-Molecule Interfaces. *Phys. Rev. Lett.* **2006**, *97*, 216405.
(76) Batra, A.; Meisner, J. S.; Darancet, P.; Chen, Q.; Steigerwald, M. L.; Nuckolls, C.; Venkataraman, L. Molecular Diodes Enabled by Quantum Interference. *Faraday Discuss.* **2014**, *174*, 79−89.
(77) Asyuda, A.; Wiesner, A.; Wan, X.; Terfort, A.; Zharnikov, M. Charge Transport Properties of Single-Component and Binary Aromatic Self-Assembled Monolayers With Methyl and Trifluoromethyl Tail Groups. *J. Phys. Chem. C* **2020**, *124*, 24837−24848.
(78) Han, Y.; Maglione, M. S.; Diez Cabanes, V.; Casado-Montenegro, J.; Yu, X.; Karuppannan, S. K.; Zhang, Z.; Crivillers, N.; Mas-Torrent, M.; Rovira, C.; Cornil, J.; Veciana, J.; Nijhuis, C. A. Reversal of the Direction of Rectification Induced by Fermi Level Pinning at Molecule−Electrode Interfaces in Redox-Active Tunneling Junctions. *ACS Appl. Mater. Interfaces* **2020**, *12*, 55044−55055.
(79) Van Dyck, C.; Ratner, M. A. Molecular Rectifiers: A New Design Based on Asymmetric Anchoring Moieties. *Nano Lett.* **2015**, *15*, 1577−1584.
(80) Kang, H.; Kong, G. D.; Byeon, S. E.; Yang, S.; Kim, J. W.; Yoon, H. J. Interplay of Fermi Level Pinning, Marcus Inverted Transport, and Orbital Gating in Molecular Tunneling Junctions. *J. Phys. Chem. Lett.* **2020**, *11*, 8597−8603.
(81) Kang, H.; Kong, G. D.; Yoon, H. J. Solid State Dilution Controls Marcus Inverted Transport in Rectifying Molecular Junctions. *J. Phys. Chem. Lett.* **2021**, *12*, 982−988.
(82) Nijhuis, C. A.; Reus, W. F.; Barber, J. R.; Dickey, M. D.; Whitesides, G. M. Charge Transport and Rectification in Arrays of SAM-Based Tunneling Junctions. *Nano Lett.* **2010**, *10*, 3611−3619.

https://doi.org/10.1021/acsphyschemau.1c00029
ACS Phys. Chem Au 2022, 2, 179−190